Research Article

Ali H. AlAteah*

Incorporating geranium plant waste into ultra-high performance concrete prepared with crumb rubber as fine aggregate in the presence of polypropylene fibers

https://doi.org/10.1515/rams-2024-0061
received May 08, 2024; accepted October 03, 2024

Abstract: This research examines the efficiency of ultra-high-performance concrete (UHPC) when utilizing geranium plant (GP) ash, which is subjected to different curing temperatures ranging from 300 to 900°C for 3 h of burning time. The GP ash is used as a replacement for cement in varying amounts (10, 20, 30, 40, and 50 wt%). Crumb rubber powder is utilized as a substitute for fine aggregate. Polypropylene fibers have been used to improve concrete performance. The performance of UHPC is evaluated by assessing its mechanical qualities, such as flexural strength, splitting tensile strength, and compressive strength. The sorptivity test is also evaluated as a component of it. Scanning electron microscopy is used to analyze UHPC after exposure to temperatures as high as 900°C. The findings demonstrated a notable enhancement in the mechanical characteristics of all mixtures. The most favorable mixtures were achieved with proportions of 50, 40, 40, and 20% for mixtures including GP waste incinerated at temperatures ranging from 300 to 900°C. Furthermore, the optimal outcome is achieved when 40% substitution is performed at a temperature of 700°C, resulting in notable enhancements of 14% in compressive strength, 30% in flexural strength, and 17% splitting tensile strength, respectively. At a high temperature of 700°C, the decrease in strength increased to approximately 37–40% as a result of the initial removal of carbon dioxide from calcite at temperatures ranging from 600 to 900°C and reached 56% at 900°C. Great resistance to sorptivity, as well as a dense and compact microstructure with a high content of calcium and silicon, was obtained.

Keywords: ultra-high performance concrete, microstructure, polypropylene fibers, concrete mechanical properties, durability, geranium waste ash

1 Introduction

Ultra-high-performance concrete (UHPC) is a composite material composed of quartz sand or river sand, quartz powder, silica fume, cement, water, and superplasticizer, which may or may not include fibers and coarse aggregates [1]. This material has been efficiently utilized in large-scale construction projects, such as high-rise buildings, bridges, and nuclear power plants. Quartz sand is a conventional aggregate used in UHPC; it is time-consuming and expensive to prepare, and its use can result in negative health effects and pollution [2,3]. Environment Canada and Health Canada (2008) reported a strong link between the increasing percentage of lung cancer in people and industries that expose them to respirable silica dust [4]. On the other hand, river sand is a non-renewable resource that is being depleted at a rate that outweighs its replenishment, which can have negative environmental impacts due to sand mining [5–7]. UHPC is a cutting-edge composite material that has revolutionized the construction industry by offering a promising alternative to traditional concrete. With its remarkable durability and strength, UHPC has advanced the development of the construction world and can be used in various applications that were previously limited by design constraints. Despite its impressive properties, the preparation of UHPC is costly because of the demand for special curing techniques, difficult manufacturing processes, and high cement content [2,8–15].

Since the 1980s, numerous researchers have used leftover tire rubber powder to create crumb rubber concrete (CRC) [16]. The incorporation of crumb rubber into

*** Corresponding author: Ali H. AlAteah,** Department of Civil Engineering, College of Engineering, University of Hafr Al Batin, P.O. Box 1803, Hafr Al Batin, 39524, Saudi Arabia, e-mail: ali.alateah@uhb.edu.sa

concrete addresses the drawbacks of its excessive weight and brittleness and expands the scope of waste rubber recycling. CRC is a composite material produced using finely ground rubber particles to replace a portion of the fine aggregate or larger rubber particles to replace a portion of the coarse aggregate in regular concrete [17]. Studies have demonstrated that CRC surpasses regular concrete in various aspects, such as energy absorption and consumption, fatigue resistance, reduction in material brittleness, deformation capacity, prevention of crack propagation, durability, and thermal performance [18]. This study focused on the use of carbon fiber-reinforced polymer (CRC) in deep foundation pit support systems to minimize the occurrence of brittle failure. Incorporating rubber powder into concrete has a positive effect on its durability and significantly reduces the rate at which chloride ions migrate within the concrete. However, the incorporation of crumb rubber resulted in a reduction in the elastic modulus, compressive strength, and tensile strength of the CRC to varying extents. The incorporation of mineral admixtures such as slag optimizes the pore structure of CRC, resulting in improved mechanical properties, particularly in terms of compressive strength [19,20]. Preheating and hardening the surface of crumb rubber enhance the compressive strength and impact resistance of CRC. Furthermore, to fully exploit the denaturation capability of CRC, many researchers have recently incorporated steel fibers into concrete to increase its impact toughness. CRC has been used in various applications, including rubber asphalt concrete pavements, CRC blocks, CRC bridge panels, flexible components, self-compacting concrete, and permeable concrete [21,22].

Recently, the accumulation of crumb rubber waste has become a significant environmental concern. Owing to the slow rate of decomposition and potential release of toxic compounds through leaching, the disposal of abandoned rubber tires and other rubber products in landfills poses a significant environmental threat [18,23]. The use of crumb rubber waste in concrete has emerged as a promising and environmentally friendly solution to this problem. By incorporating crumb rubber into concrete mixtures, researchers can reduce the amount of rubber waste in landfills and improve the durability and flexibility of the resulting concrete [18,21,24]. This innovative approach provides a mutually beneficial solution for both the environment and the construction industry by not only reducing the negative impact of discarded rubber but also creating a stronger and more environmentally friendly building material for various infrastructure projects [16,25,26]. The incorporation of crumb rubber in concrete as a method of recycling sand represents a novel and sustainable approach to waste reduction and enhancement of construction materials [19]. This innovative idea involves combining sand, a readily available material, with crumb rubber, a waste product derived from discarded tires. This environmentally conscious approach not only reduces the reliance on virgin sand, which is commonly extracted in excessive amounts from natural sources, but also confers several beneficial characteristics to the resulting concrete. These include increased flexibility and resilience, which leads to improved resistance to cracking and impact damage, reduced noise levels within buildings, and enhanced insulation [18,27,28]. In conclusion, the process of recycling sand with crumb rubber in concrete not only conserves natural resources but also results in a flexible and environmentally friendly building material that aligns with the principles of sustainability and circular economy.

Agricultural waste is commonly utilized in the concrete industry [29,30], particularly in the production of various types of concrete, such as lightweight, geopolymer, and reactive powder concrete [31–33]. Several agricultural waste materials, including corn ash [34,35], cotton husk ash [36,37], sugar cane bagasse ash [38–41], rice straw ash [42–46], palm oil ash [47–50], and rice husk ash [19–23], have been incorporated into concrete to enhance its performance [51–53], particularly in geopolymer concrete, reactive powder concrete, and lightweight concrete, with a significant role in the pozzolanic reaction [36,51,54–65], particularly in lightweight and geopolymer concrete. By burning agricultural waste at high temperatures, it is possible to improve its chemical properties such as compressive strength, tensile strength, and flexure strength. For instance, sugar cane bagasse ash precured at temperatures ranging from 200 to 800°C for 2 h with increasing silica content from 75%, 17.78 MPa, and 24.05 MPa in compressive strength, tensile strength, and flexure strength, respectively [35]. Similarly, rice husk ash was used in UHPC mixes after burning at different temperatures, and it significantly improved UHPC performance when heated at 500°C for 2 h, resulting in a 9.7% at 7 days, 14.5% at 28 days, and 10.2% at 120 days improvement in compressive strength, respectively, when cement content was replaced by 2/3 of its value by rice husk ash [66]. Geraniums have a significant presence in the realm of decorative plants, and their widespread availability in the flower industry is well established [67,68]. In urban settings, they are commonly used in a variety of contexts, such as flower beds, containers, and green spaces, and are renowned for their ability to thrive under harsh environmental conditions. Furthermore, geraniums exhibit the unusual characteristic of becoming organic heavy metal accumulators, which makes them useful in phytoremediation for removing or reducing contaminants from contaminated soil or water. Geranium waste, which includes discarded leaves, stalks, flowers, and other plant parts, is the byproduct or residue of geranium cultivation, processing, or disposal and is sometimes considered trash. However, this waste has significant value and can be used for various purposes. For instance, it can be composted to produce organic fertilizers that support sustainable agriculture. Additionally, geranium waste can be recycled to create essential oils and natural colors that have applications in the perfume, cosmetics, and herbal medicine sectors. Furthermore, the natural heavy metal acquisition property of geraniums makes their waste materials suitable for phytoremediation uses, which support the remediation of damaged soils or waters. By exploring innovative ways to utilize geranium waste, we can unlock its potential and encourage a more circular and sustainable approach to geranium cultivation [69].

1.1 Research significance

The literature review revealed that previous studies had examined the feasibility of incorporating different agricultural and industrial waste materials into UHPC. However, the objective of this study is to develop environmentally friendly UHPC by substituting a portion of the cement with geranium plant waste (GPW) powder. This substitution is a viable and sustainable alternative for cement, offering practicality and user-friendliness. In addition to saving natural resources of sand by using alternative resources and solving environmental problems of landfills, no specific investigation has been conducted on the effects of incorporating geranium waste or perfume industry waste in concrete. This is especially pertinent considering the present climatic and environmental concerns regarding carbon emissions, as well as the increasing abundance of various industrial waste materials and scarcity of natural resources. Moreover, the worldwide expense of garbage disposal is escalating, necessitating the development of sustainable alternatives.

2 Experimental work

2.1 Raw materials

This investigation employed conventional Portland cement 52.5N, which adhered to the BSEN197/1 2011 standard [70]. The Sika Company in Egypt manufactured silica fume with a specific gravity of 3.15 and a surface area of 3,960 $cm^2{\cdot}g^{-1}$, as well as silica fume with a surface area of 200,000 $cm^2{\cdot}g^{-1}$, a specific gravity of 2.13, and a density of 0.78 $g{\cdot}cm^{-3}$. The silica fume had an initial setting time and a final setting time of 134 and 198 min, respectively, and exhibited compressive strengths of 24.2 MPa at 7 days and 52.5 MPa at 28 days. Table 1 shows the chemical composition of cement and silica fume. The GPW used in the experiment was obtained from a perfume-manufacturing company and subjected to a drying process at a temperature of 25°C, followed by heating in an oven for burning for 3 h at varying rates of 10°C per min, reaching temperatures ranging from 300 to 900°C with 200°C step. The heated samples were then crushed and passed through a 90 mm screen, and their chemical compositions were analyzed using EDEX analysis. A sample of crumb rubber was used as a fine aggregate of bulk density and specific gravity of 530 $kg{\cdot}m^{-3}$ and 0.97, respectively. Figure 1 shows a sieve analysis diagram for rubber; the Sika Company provided polypropylene fiber and a third-generation superplasticizer named SikaViscoCrete5930, which has a pH range of 8.0–1.0 and a density of 1.08 $kg{\cdot}m^{-3}$. Figure 2 illustrates the raw materials used for the UHPC production (Figure 3).

2.1.1 GPW preparation steps

Geranium waste ash was acquired from nearby agricultural establishments, and meticulous efforts were made to gather the ash while eliminating any undesired clumps or debris. The ash was subsequently incinerated in a furnace at 300, 500, 700, and 900°C for 3 h at a heating rate of 10°C·min^{-1} after reaching the target temperature; the samples were kept for 3 h and then cooled to ambient temperature in the oven to avoid oxidation when subjected to air. Following the heating process, the ash was cooled to room temperature for 1 h. Subsequently, the samples were crushed using a zirconia ball mill for 30 min to obtain a particle size of 90 µm (Figure 4). The ashes were subsequently sifted and satisfied the precise requirements specified in BS 3892: Part 1–1997 and ASTM.

Table 2 presents the X-ray fluorescence analysis results of the geranium waste, indicating that the ash had a micro-sized structure. The ashes were subsequently utilized as a substitute for cement in varying ratios (10–50 wt%) to conduct a comprehensive analysis of their properties. The results were determined to comply with the specifications established by BS 3892: Part 1–1997 and ASTM.

2.2 Concrete mix design

To achieve the desired properties of UHPC (high strength, impermeability, low porosity, and high density), an appropriate w/c ratio was selected, as shown in Table 2 [71]. Several

Table 1: Chemical composition of cement and silica fume (%)

Chemical composition (%)	SiO_2	Al_2O_3	Fe_2O_3	CaO	MgO	K_2O	Na_2O	SO_3	Cl	Free lime
CEM I	20.97	5.65	2.41	64.88	2.68	0.6	—	2.81		
SF	98.1	0.11	0.15	0.11	0.3	1.1	0	0.13		

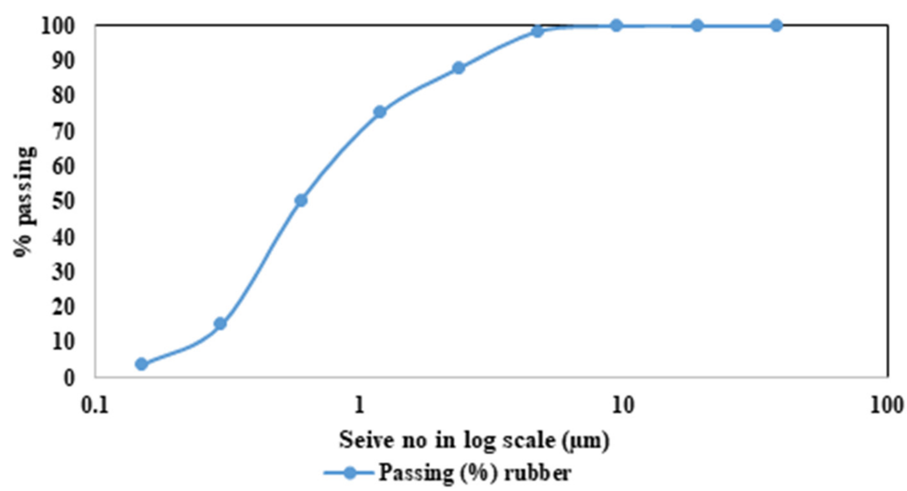

Figure 1: Sieve analysis for waste rubber.

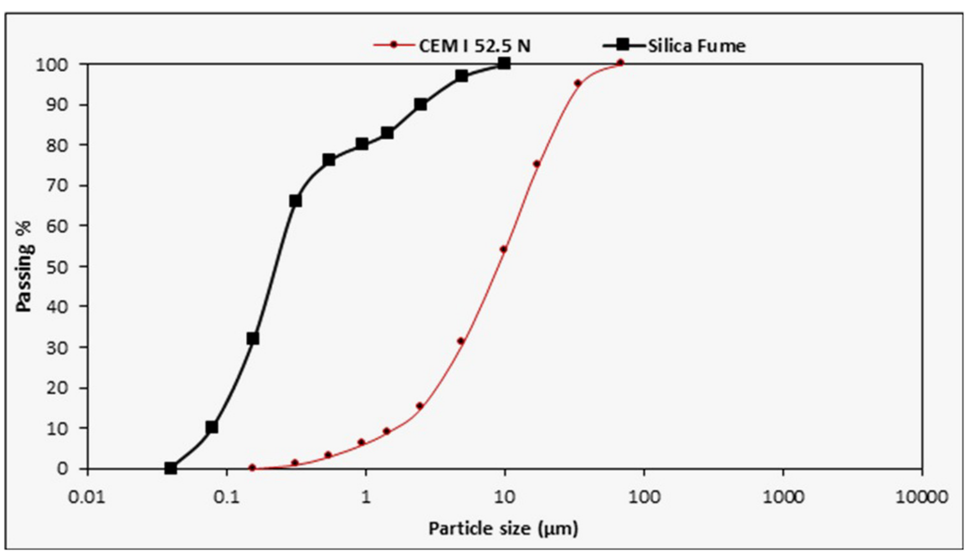

Figure 2: Sieve analysis for cement and silica fume.

experimental trials were conducted to accurately satisfy UHPC standards. After obtaining the target strength, geranium waste at various percentages, including 10–50 wt% of cement, was replaced from cement content. Finally, polypropylene fiber was added and mixed to avoid the balling effect. The mixing proportions are shown in Table 3.

2.3 Mixing procedures

The mixing ratios required for UHPC are detailed in Table 2. The packing density theory for UHPC was achieved through a series of tests that followed the Andreasen and Andersen model [72] as follows.

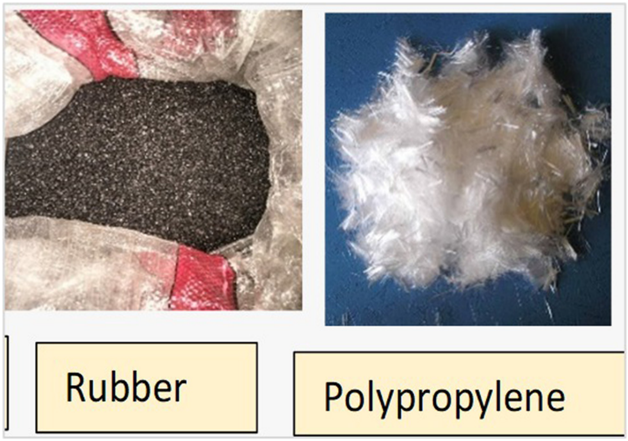

Figure 3: Rubber and polypropylene appearance.

Mixing procedures involved combining dry binders, such as silica fume, cement, and GPW, in a mixer for 120 s at a low speed. This was followed by the addition of superplasticizer and water, and the components were then mixed for an additional 2 min at a low speed, and then a homogeneous composite was obtained by mixing for 3 min at a high speed. In total, 21 mixes were prepared: one control mix and five mixes prepared for each burning degree with dosages of 10, 20, 30, 40, and 50%. The samples were then compacted and allowed to cure in a laboratory environment for 24 h [73].

2.4 Casting and curing

A concrete mixer with a capacity of 10 L was used for the mixing process. To ensure a consistent mixture, cement, sand, and silica fume were precisely measured before being combined. The superplasticizer and water were mixed in a separate container and then added to the dry ingredients in the mixer drum. The mixture was carefully blended to achieve ideal consistency for casting. The time required for various components to combine varied for each mixture. We created cylindrical specimens with a diameter of 100 mm and a height of 200 mm, as well as cubic specimens with dimensions of 100 mm for each concrete mixture.

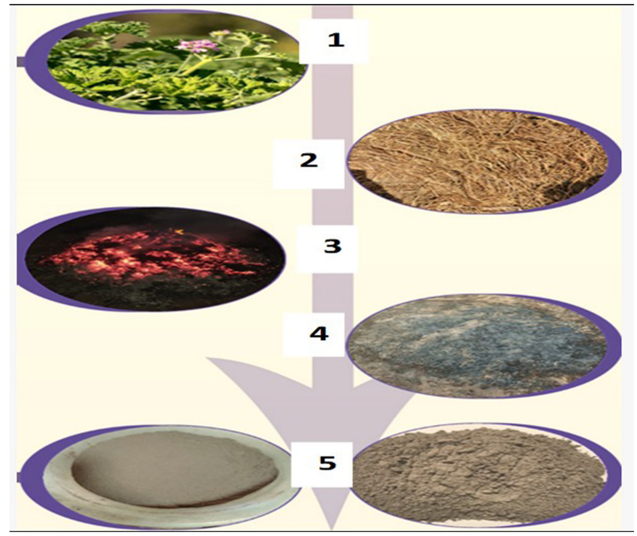

Figure 4: Preparation process for geranium waste powder before burning at elevated temperatures.

The molds were gently vibrated to release any trapped air before each of the three concrete layers was placed inside. Plastic sheets were placed over the specimens after the concrete surface was finished to prevent water evaporation. After a 48-h interval, the specimens were removed from the molds and immersed in a water tank maintained at a constant temperature of 25°C/2°C until testing ages of 7, 28, and 90 days for compressive strength.

3 Testing

The investigation included examining the mechanical properties, durability, and microstructure of the concrete mixes at room temperature, as well as conducting compressive strength tests at high temperatures. Some samples were used to evaluate the compressive strength, and the specimens were tested using an ELE crushing machine with a capacity of 3,000 kN, with a loading rate of 6.8 $kN \cdot s^{-1}$ in accordance with ASTM C109, BS EN 12390 3:2019, and other standards. The specimens were subjected to compressive strength testing at ages of 7, 28, and 90 days, as well as at

Table 2: Chemical composition of GPW after different treatment methods (%)

Chemical composition (%)	SiO_2	Al_2O_3	Fe_2O_3	CaO	MgO	K_2O	Na_2O	SO_3	Cl	Free lime
(GPW) 300	46.37	4.87	13.1	16.09	5.01	3.86	2.68	1.35	1.73	2.33
(GPW) 500	49.09	5.97	13.2	15.36	3.48	3.06	3.54	1.36	1.83	1.15
(GPW) 700	51.63	6.49	13.83	15.43	3.55	3.67	2.11	1.11	1.17	1.01
(GPW) 900	53.82	7.12	14.27	13.2	3.82	3.18	2.34	1.16	0.21	0.88

Table 3: Mix proportions (kg·m^{-3})

	c	GP%	SF	CR	SP%	w	w/c	PP
C100G0	900	0	240	1,150	1.5	150	0.16	0.9
10G300	810	90	240	1,150	1.5	150	0.16	0.9
20G300	720	180	240	1,150	1.5	150	0.16	0.9
30G300	630	270	240	1,150	1.5	150	0.16	0.9
40G300	540	360	240	1,150	1.5	150	0.16	0.9
50G300	450	450	240	1,150	1.5	150	0.16	0.9
10G500	810	90	240	1,150	1.5	150	0.16	0.9
20G500	720	180	240	1,150	1.5	150	0.16	0.9
30G500	630	270	240	1,150	1.5	150	0.16	0.9
40G500	540	360	240	1,150	1.5	150	0.16	0.9
50G500	450	450	240	1,150	1.5	150	0.16	0.9
10G700	810	90	240	1,150	1.5	150	0.16	0.9
20G700	720	180	240	1,150	1.5	150	0.16	0.9
30G700	630	270	240	1,150	1.5	150	0.16	0.9
40G700	540	360	240	1,150	1.5	150	0.16	0.9
50G700	450	450	240	1,150	1.5	150	0.16	0.9
10 G900	810	90	240	1,150	1.5	150	0.16	0.9
20G900	720	180	240	1,150	1.5	150	0.16	0.9
30G900	630	270	240	1,150	1.5	150	0.16	0.9
40G900	540	360	240	1,150	1.5	150	0.16	0.9
50G900	450	450	240	1,150	1.5	150	0.16	0.9

c: cement, GP: geranium plant, PP: polypropylene fiber, SF: silica fume, w: water, SP: superplasticizer.

elevated temperatures of 300, 500, 700, and 900°C, while the other specimens were heated in an electric furnace at a heating rate of 10°C·min^{-1} to the target temperature. When the desired temperature was achieved, it was maintained constant for 2 h. Subsequently, the furnace was cooled at a rate of 1.67°C·min^{-1} to avoid any thermal shock to the specimens. Cylindrical specimens with dimensions of 100 mm × 200 mm were tested for splitting tensile strength in accordance with ASTM C496, and 100 mm × 100 mm × 500 mm beams were used to investigate the flexural strength. For each mixture, three specimens of each age were cast and cured until the testing date, and the average strength was calculated. Nine cubes of each mix were cast for 7, 28, and 90 days, in addition to three cylinders for each mix for splitting at 28 days and three beams for flexure at 28 days. For durability evaluation, a sorptivity test was performed on all mixes using cylinders of 100 mm diameter × 50 mm length after drying the samples at 105°C, as per ASTM C1585. Microstructure analysis was performed using a scanning electron microscope on thin sections taken from crushed cube cores, in addition to thermogravimetric analysis (TGA), to determine the effect of GPW on the decomposition of internal hydration products [74].

4 Results and discussion

4.1 Compressive strength

A compressive strength test was conducted on all the designed mixtures to assess the performance of UHPC that incorporated GPW that had been burnt at 300–900°C. The goal is to compare their performance and determine the most suitable choice with the best performance and optimal dosage. Figure 5a shows the compressive strength of UHPC incorporating GPW burnt at 300°C. The results indicated that replacing the cement weight with GPW increased the compressive strength at all ages for all dosages. Moreover, it is clarified that there is compatibility in the trend of CSH findings at all ages, where the CSH outcomes are boosted gradually up to a replacement ratio of 40%. The compressive strength of the mix gradually increased from 110 MPa at the reference mix to 116 MPa at 40% and then decreased to 114 MPa at the age of 7 days. Compared to the control mix with zero waste (GP), the compressive strength increased from 131 MPa for the reference mix to 139.8 MPa at 28 days and from 140 MPa for the control mix at 90 days to 148 MPa with increasing ratios ranging between 4 and 7% at all ranges. Figure 3b shows similar results for GP burnt at 500°C. Replacing cement with GPW has a positive effect on the compressive strength results at all replacement ratios up to 10% at 7 days, with a significant increase in compressive strength from 110 to 120 MPa at a 40% replacement ratio and a small decrease at a 50% replacement ratio of 119 MPa. The same trend was obtained at 28 and 90 days with an increase rate of 8.7%. In general, it was observed that a 40% replacement ratio achieved the best performance for this group. When the cement was replaced with GPW treated at 700°C, the strength increased dramatically up to a 50% replacement ratio, and the strength increased (1) from 110.2 to 125 MPa at 7 days and (2) from 131.2 to 150 MPa at 28 days, owing to high pozzolanic reactions, which may have occurred because of the silica content of 51.3% that can react with calcium hydroxide, resulting in CSH. Moreover, the silica content in GPW is approximately 2.5 times greater than that in cement, and the fineness of the particles also participates in the production of CSH. At the age of 90 days, the strength increased for all mixes gradually from 140 to 158 MPa, achieving the optimum dosage, as shown in Figure 5c. Figure 5d displays the compressive strength when GPW powder treated at 900°C was utilized. The results indicate that adding GPW improves the compressive strength up to a 20% replacement ratio, and after 20%, the compressive strength decreases gradually, reaching a strength greater

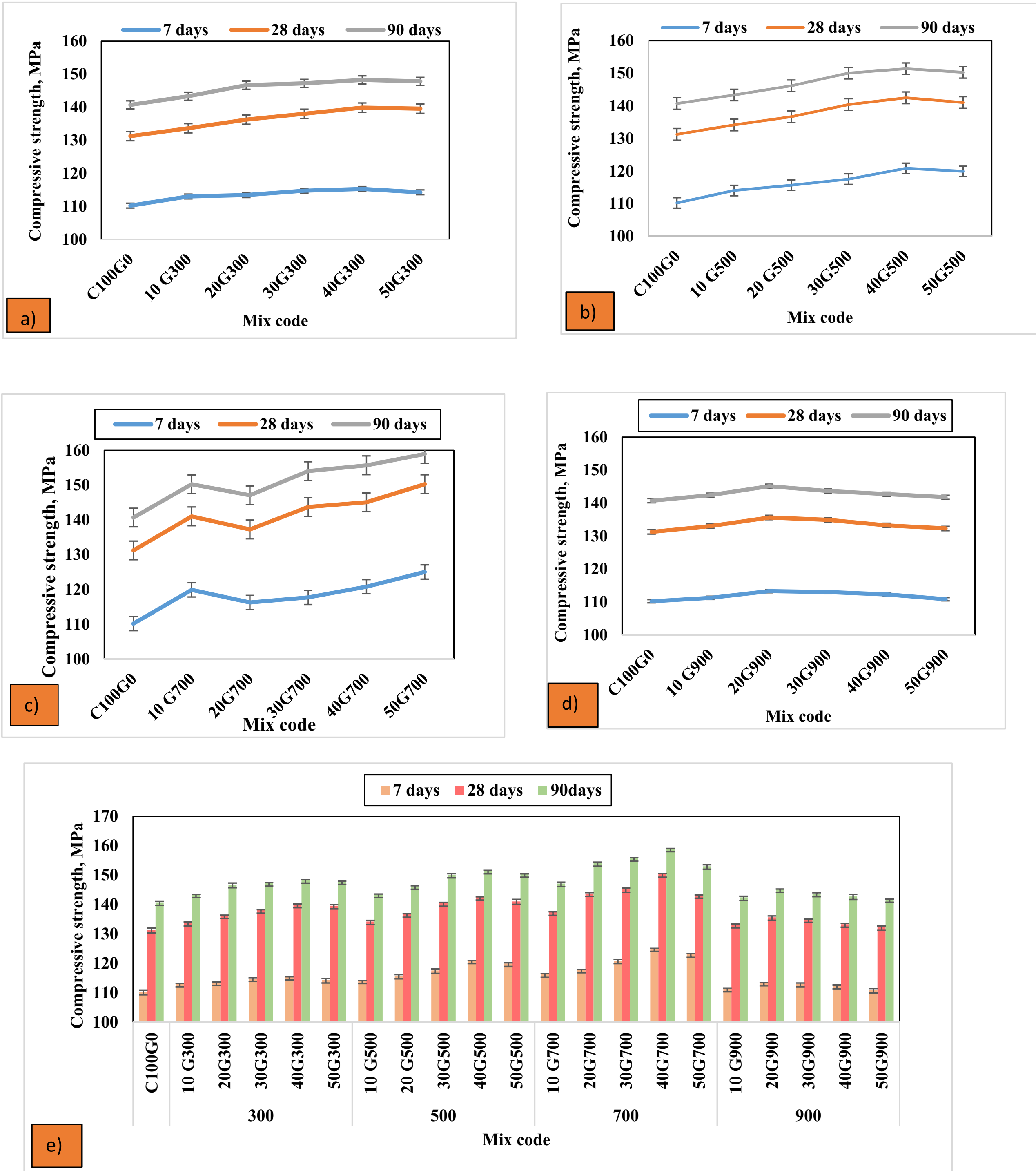

Figure 5: Compressive strength for UHPC incorporating GP waste: (a) 300°C, (b) 500°C, (c) 700°C, (d) 900°C, and (e) cumulative curve for all burning degrees.

than that of the control mix. However, the decrease in the optimum value may be due to the presence of unreacted silica in the composition of GPW when subjected to 900°C and higher contamination.

Figure 5e explains the cumulative figure for compressive strength for 21 different dosages and GPWs. It can be concluded that burning GPW at 700°C is the best compared to the studied temperatures, achieving a 19% increase in strength with decreasing cement content by 320 kg·m^{-3}. The strength improvement of the mixes with GPW treated at 900°C can be attributed to the insufficient calcium hydroxide needed to react with the high silica content present in GPW or the negative effect of temperatures higher than 700°C, which improves the crystalline phase of silica and decreases the pozzolanic reaction continuity. In addition, specific areas play an important role in accelerating reactions.

4.2 Split tensile strength

The aim of this study is to evaluate the indirect tensile strength of different mixtures through the implementation of a splitting tensile strength test on cylindrical specimens with dimensions of 100 mm × 200 mm. The results depicted in Figure 6 demonstrate a notable augmentation in the splitting strength for all mixtures incorporating GPW, along with a substantial value for the reference mixture attributed to the reinforcing effect of the polypropylene fibers. Throughout the testing procedure, initial observations revealed the emergence of minor fractures, and at the point of maximum load on the bearing, the samples experienced a total division into two separate halves [75–77]. A study was conducted to assess the indirect tensile strength of different mixtures by subjecting cylindrical specimens measuring 100 mm × 200 mm to a splitting tensile strength test. The objective of this study was to evaluate the efficacy of incorporating polypropylene fibers with GPW. As shown in Figure 3, all the mixtures incorporating GPW exhibited a notable enhancement in the splitting strength. The reference mixture also showed a high starting value, which is attributed to the reinforcing influence of the polypropylene fibers. During the test, the first microfractures were observed, and at the point of maximum force, the samples experienced a complete fracture, resulting in two separate halves. The findings demonstrated that the adhesion between the geranium powder and UHPC constituents improved the interfacial transition zone (ITZ), resulting in heightened strength. Furthermore, the substitution of cement with fine materials abundant in amorphous silica also played a role in increasing the strength. As presented in Figure 3, the splitting tensile strength increased by 8.3–21.3% for mixes 10G300-50G300, 8–21% for mixes 10G500-40500, 11.7–27.8% for mixes 10G700-40G700, and 10–16% for mixes 10G900-20G900. The most favorable outcomes were achieved at varying temperatures for the treatment of GPW, which aligns with the findings on compressive strength.

4.3 Flexural strength

The flexural strength of 21 mixtures is assessed using the four-point test to evaluate the performance of various mixtures. The addition of GPW (GP as a replacement for cement significantly impacts the flexural strength of UHPFC). The use of GP was found to significantly improve the flexural strength of UHPC [58], and all mixtures incorporating GPW achieved a high degree of flexural strength similar to that of the reference mixture. The failure strength is related to the ultimate phase, during which cracks appear in the samples under stress. As the weight increased, the cracks in the specimens expanded and elongated, eventually joining together and strengthening the central area. Eventually, there was a failure in the form of a vertical crack [78]. The use of GPW in place of cement resulted in varying increases in flexural

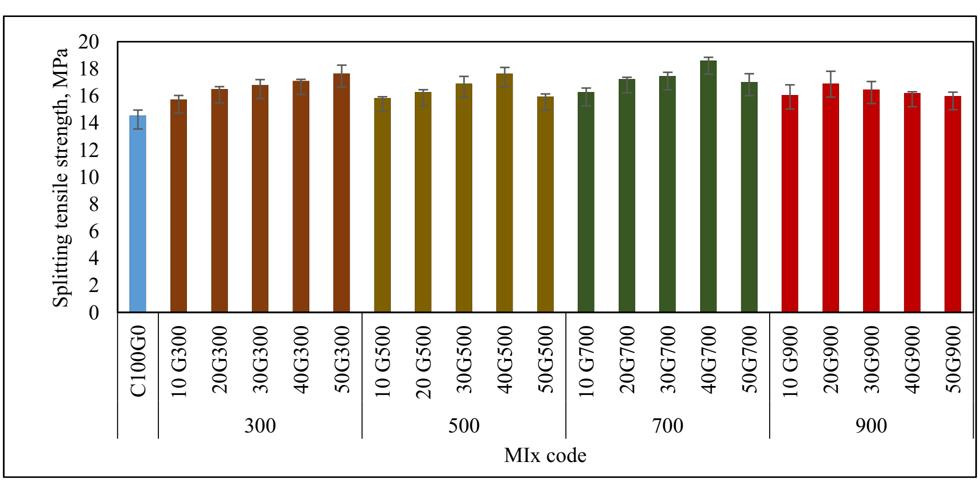

Figure 6: Splitting tensile strength for UHPC with GPW.

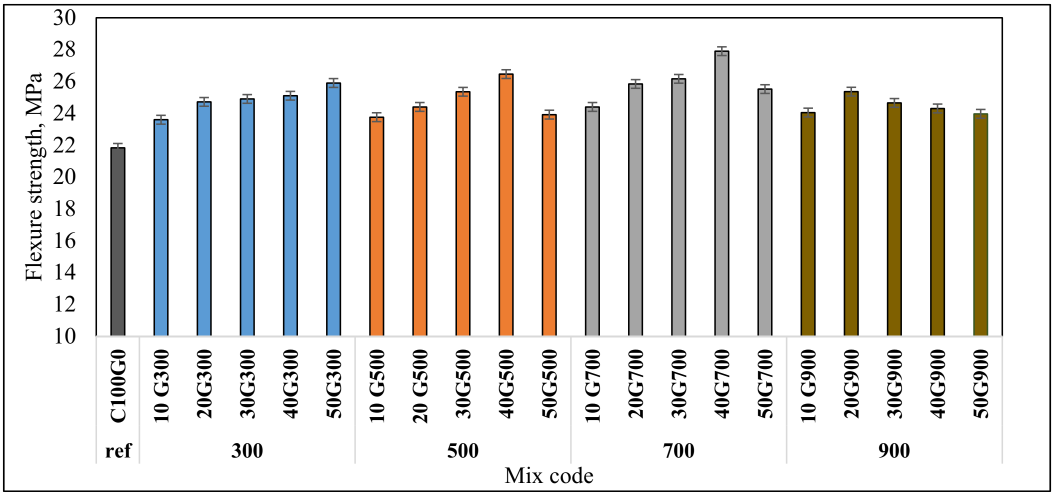

Figure 7: Flexure strength for UHPC contains GPW.

strength: 18% at 50% GP prepared at 300°C, 18% at 40% replacement ratio prepared at 500°C, 30% increase at 40% replacement dosage pretreated at 700°C, and 13.6% at 20% replacement of GP treated at 900. The mixes incorporating GPW exhibited a flexural strength of 28 MPa, which surpassed the value of 22 MPa achieved in the absence of GPW. The exceptional flexural strength of UHPC can be attributed to its compact microstructure and robust ITZ between the aggregate and matrix, as illustrated in Figure 7.

4.4 Sorptivity

The GPW ash functions as a physical micro-filler, efficiently filling the voids between cement particles. The sorptivity of the concrete diminishes due to the constraining effect of the fine powder on water penetration. Consequently, the reduced porosity restricts the absorption of water through the capillaries, thereby further decreasing the sorptivity [8,63]. Figure 8 illustrates a progressive rise in sorptivity resistance, varying from 4.6 to 18%, for mixtures with a gradation of 10G300–50G300. In the same manner, blends with a range of 10G500–50G500 showed an increase from 7.5 to 18.6%. Significantly, the mixes with a range of 10G700–50G700 showed a notable increase from 19.18 to 43.3%. Finally, the mixtures ranging from 10G900 to 50G900 exhibited a progressive rise in percentage, increasing from 4.6 to 17.5%. Consequently, the addition of GP improved the concrete performance by decreasing its porosity, thereby enhancing its resistance to absorption [8,10]. The incorporation of GPW also led to a substantial decrease in the sorptivity. Various factors have

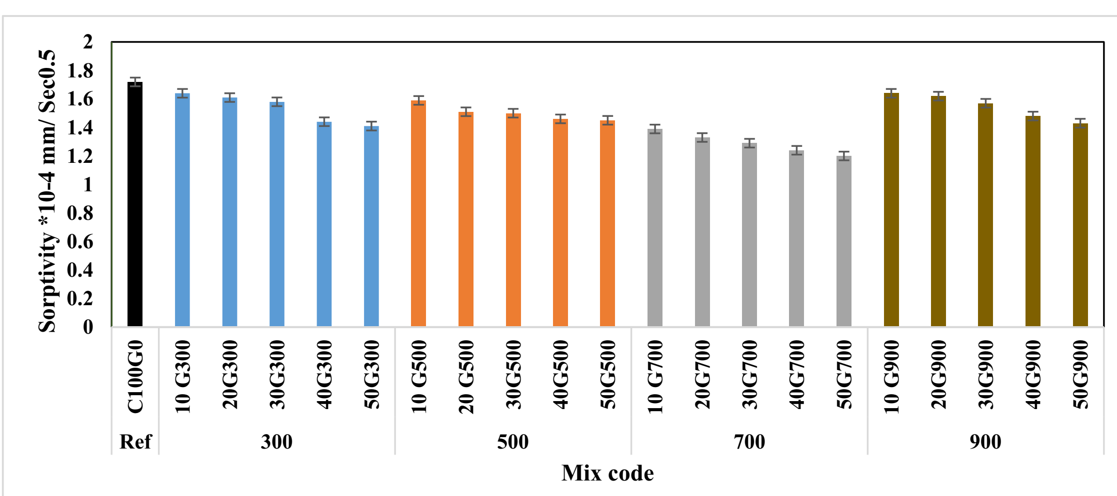

Figure 8: Sorptivity for UHPC incorporating GPW.

contributed to this decline. By introducing GPWs, the compaction of the concrete mixture was first improved. This leads to a denser matrix with fewer vacant spaces that are interconnected, hence decreasing the number of paths for water to penetrate [8,10,63]. This enhanced packing diminishes the rate of moisture absorption by the material. Furthermore, GP residues exhibit pozzolanic characteristics, signifying their capacity to undergo chemical reactions with calcium hydroxide (CH) and produce supplementary cementitious compounds. This chemical reaction causes the microstructure to become more tightly packed, causing a significant lowering in the porosity of the concrete.

4.5 Compressive strength after subjecting to elevated temperatures

The loss in compressive strength of 21 mixes of four groups of ultra-high-performance fiber-reinforced concrete (UHPBFC) with varying dosages of cement replacement (10, 20, 30, 40, and 50 wt%) using GPWs and rubber as fine aggregate are shown in Figure 9. The specimens were dried at 100°C and then heated to 300, 500, 700, and 900°C for 3 h. Three cubes were selected and subjected to different temperatures for testing, and their compressive strengths were measured. The findings indicated a marginal enhancement in compressive strength upon subjecting the samples to 100°C, followed by a progressive decline in strength as the temperature increased to 900°C. Some reactions occurred, beginning with the removal of water bound to other substances at 100°C, resulting in a decrease in moisture. As a result, there was a minor increase in the compressive strength of approximately 5% for all mixtures. Thermal strain can occur at 300°C when the dihydroxylation of CSH occurs within a temperature range of 150–400°C. This process led to the formation of microcracks [79–81]. Moreover, the compressive strength experienced a decrease of roughly 7–11% as the temperature increased up to 500°C. Rising temperatures can result in thermal expansion as well as the formation of internal fissures, which ultimately weaken the material's structural integrity. The dehydration of CH at temperatures ranging from 400 to 600°C resulted in a significant strength reduction, measuring approximately 28%, and caused the disintegration of the microstructure of the material [82,83]. At a temperature of 700°C, the decrease in strength increased to around 37–40% as a result of the initial removal of carbon dioxide from calcite at temperatures ranging from 600 to 900°C and reached 56% at 900°C. The average strength of polypropylene fibers undergoes the following changes at different temperatures: an increase of up to 5.8% at 100°C, 10.8% at 300°C, 28% at 500°C, 38% at 700°C, and 56% at 900°C over a 3-h period. This suggests that UHPBFC has a greater resistance to heat when exposed to high temperatures [84].

4.6 TGA

TGA is performed for all mixes, and results in Figures 10 and 11 show that TGA for UHPC incorporating GPW treated at different temperatures achieved increasing weight loss due to CSH decomposition due to more pozzolanic

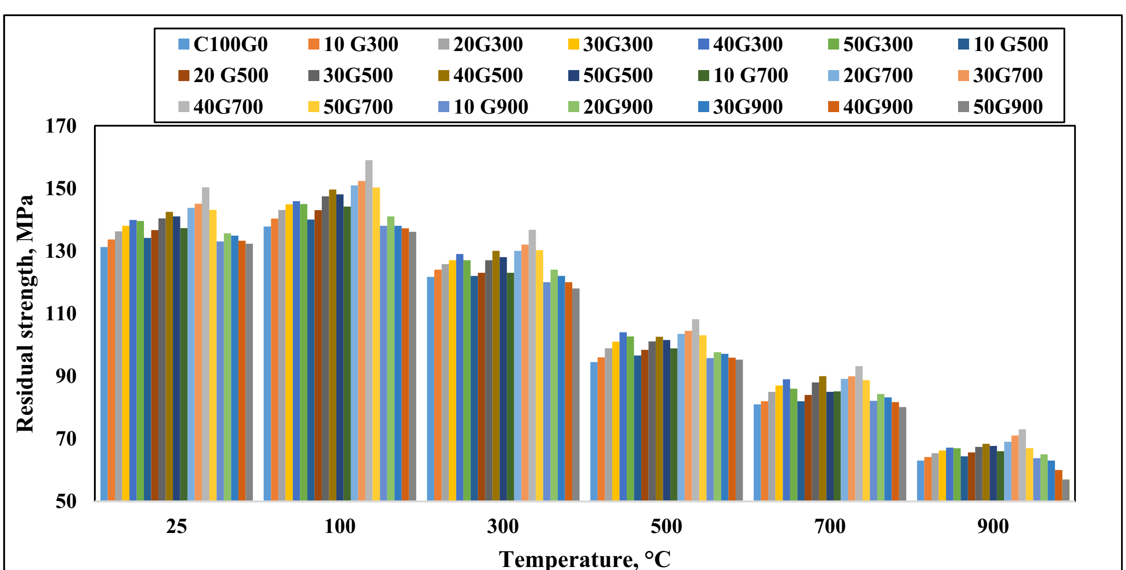

Figure 9: Compressive strength after subjecting to elevated temperatures for GP blended UHPBFC.

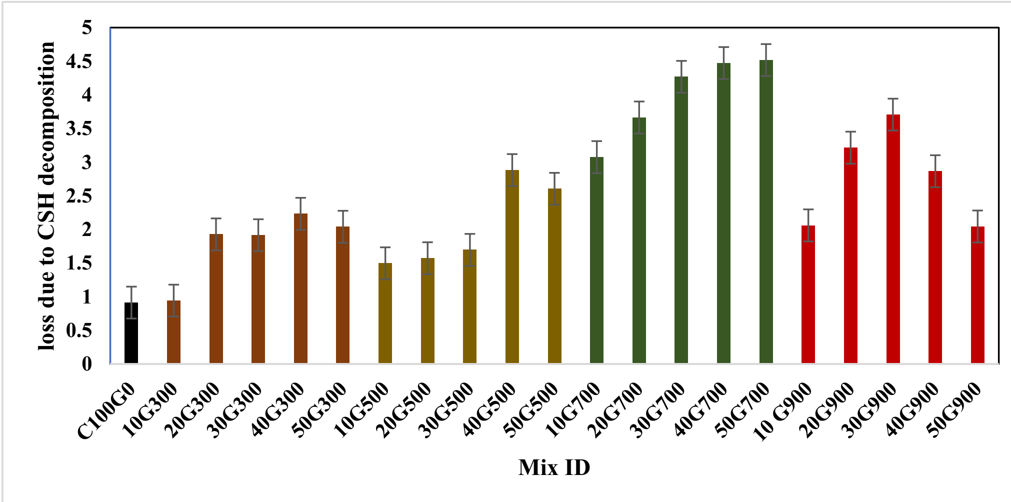

Figure 10: Mass loss due to CSH decomposition.

reactions. By adding GPW to UHPC, organic components are introduced that undergo pozzolanic interactions with the cementitious matrix, especially when exposed to high treatment temperatures. TGA studies commonly show an augmentation in weight reduction, primarily ascribed to the dissolution of calcium silicate hydrate (C-S-H) phases in the concrete. The degradation observed here suggests an increase in the pozzolanic activity, as the treated geranium waste combines with the calcium hydroxide in the concrete to produce more C-S-H. This reaction not only utilizes the lime that would otherwise not react, but also enhances the microstructure of the concrete, so improving its overall durability and performance. The weight loss observed in TGA curves, which increases as the treatment temperature of the plant waste increases, serves as a quantitative indication of the magnitude of these pozzolanic processes and their influence on the thermal stability of the composite material.

4.7 Microstructural assessment

In this study, a scanning electron microscopy (SEM) analysis was performed to evaluate the mechanical properties of five compositions cured at room temperature. The primary objective of this study is to investigate the effects of replacing cement with ground palm kernel shell (GP) as an

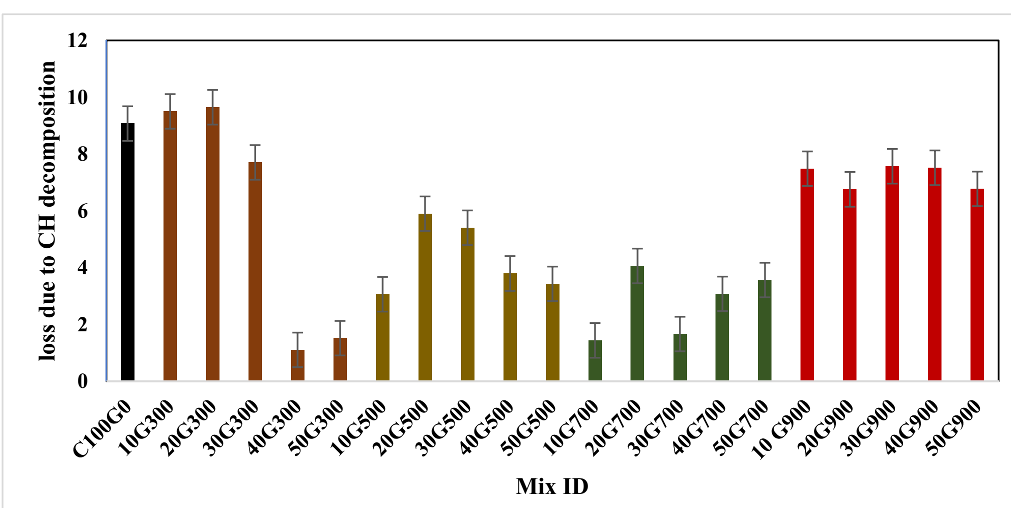

Figure 11: Mass loss due to CH decomposition.

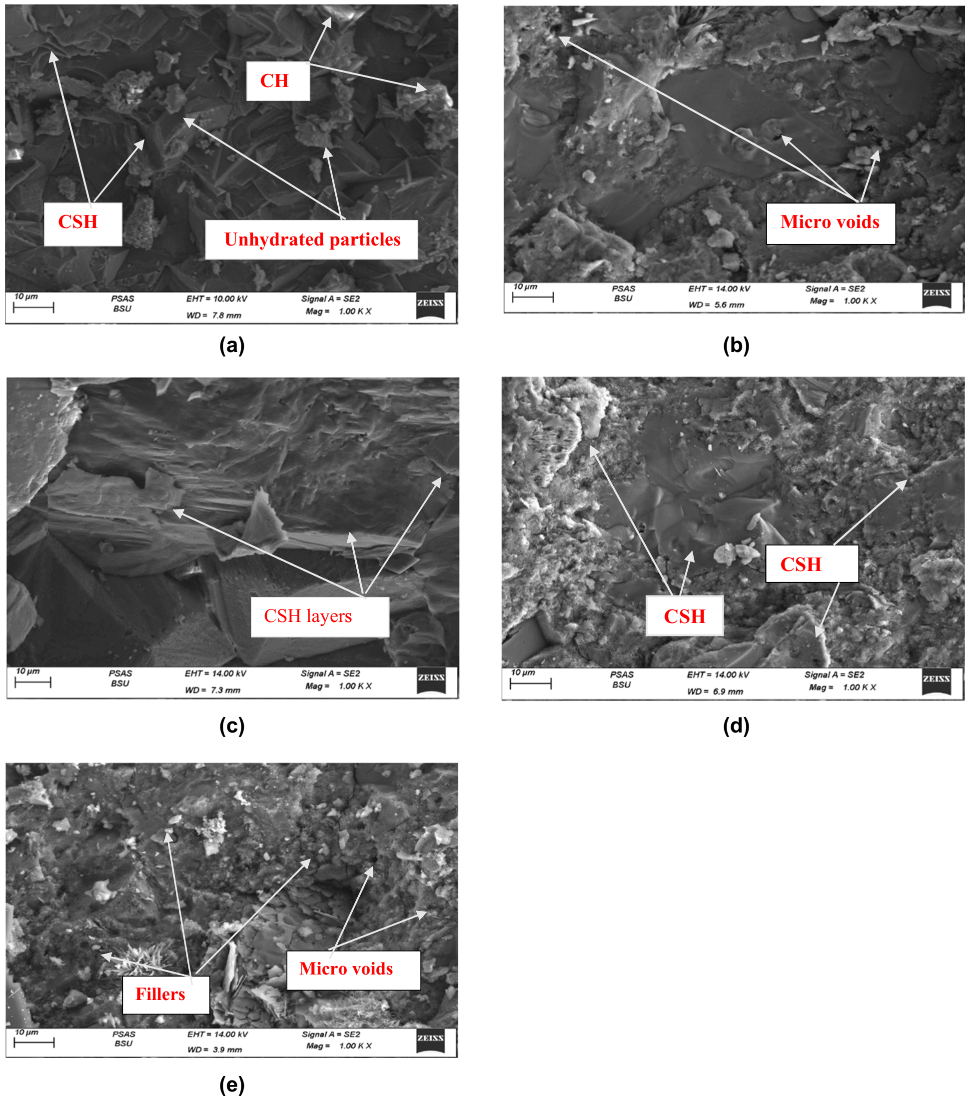

Figure 12: SEM micrograph of UHPC. (a) SEM micrograph for reference mix. (b) SEM micrograph for 50GP300. (c) SEM micrograph for 40% GP prepared at 500. (d) SEM micrograph for 40% GP prepared at 700. (e) SEM micrograph for 20% GP prepared at 900.

aggregate. The SEM images of the five samples with optimum compressive strength are shown in Figure 12a–e. These images reveal a highly compact structure with minimal gaps and cracks, which can be attributed to the increased packing density achieved using GP as an aggregate that exhibits a uniform distribution [85–87], combined with a robust ITZ and a powder [88,89]. The incorporation of GPW increased the pozzolanic process, resulting in the formation of a CSH gel [89].

5 Conclusion

This research investigates the performance of UHPC by replacing GPW burnt at temperatures of 300, 500, 700, and 900°C with varying proportions of waste (10, 20, 30, 40, and 50%) relative to the weight of cement to achieve environmental aspects. An investigation was conducted on the mechanical properties, including compressive strength, splitting, durability, and microstructure. The results of this study are presented as follows:

- The compressive strength exhibited a significant increase in all mixes containing a higher proportion of GPW compared to the control mix.
- The most favorable proportions were achieved by substituting 50% at 300°C, 40% at 500°C, 40% at 700°C, and 20% at 900°C of GPW at temperatures of 300, 500, 700, and 900°C, respectively.
- The splitting tensile strength of all the mixes improved when different replacement ratios were used. The

optimal strength increased when 40% of the GPW burnt at a temperature of 700°C was used. Additionally, there was significant improvement in the flexural strength.
- The addition of GPW led to a significant reduction in the sorptivity. Multiple factors contribute to this decrease. Initially, the compaction of the concrete mixture was enhanced by incorporating GPWs, resulting in a more compact matrix with fewer interconnected empty spaces.
- SEM analysis of UHPC, including ground granulated blast furnace slag (GPW), conducted at room temperature exhibited a finely tuned and densely packed microstructure. Fine GPW particles fill the voids, resulting in a denser matrix with improved particle packing. Enhanced adhesion is achieved by optimizing the interface between the cementitious matrix and aggregate network, resulting in a stronger binding strength.
- The inclusion of ground granulated blast furnace slag (GPW) in UHPC enhances its microstructural integrity and thermal stability, making it a promising material for high-temperature applications.

Acknowledgments: The author acknowledges the facilities and support provided by the University of Hafr Al Batin, Saudi Arabia.

Funding information: The author states no funding involved.

Author contributions: The author has accepted responsibility for the entire content of this manuscript and approved its submission.

Conflict of interest: The author states no conflict of interest.

Data availability statement: The datasets generated and/or analyzed during the current study are available from the corresponding author on reasonable request.

References

[1] Yu, Z., L. Wu, Z. Yuan, C. Zhang, and T. Bangi. Mechanical properties, durability and application of ultra-high-performance concrete containing coarse aggregate (UHPC-CA): A review. *Construction and Building Materials*, Vol. 334, 2022, id. 127360.

[2] Yu, R., P. Spiesz, and H. J. H. Brouwers. Development of an eco-friendly Ultra-High Performance Concrete (UHPC) with efficient cement and mineral admixtures uses. *Cement and Concrete Composites*, Vol. 55, 2015, pp. 383–394.

[3] Chen, Z., J. Yu, Y. Nong, Y. Yang, H. Zhang, and Y. J. C. S. Tang. Beyond time: Enhancing corrosion resistance of geopolymer concrete and BFRP bars in seawater. *Composite Structures*, Vol. 322, 2023, id. 117439.

[4] Abellán-García, J. Four-layer perceptron approach for strength prediction of UHPC. *Construction and Building Materials*, Vol. 256, 2020, id. 119465.

[5] Younis, S. A., E. M. El-Fawal, and P. Serp. Nano-wastes and the environment: potential challenges and opportunities of nano-waste management paradigm for greener nanotechnologies. *Handbook of environmental materials management*, 2018, pp. 1–72.

[6] Nandhini, K. and J. Karthikeyan. Sustainable and greener concrete production by utilizing waste eggshell powder as cementitious material – A review. *Construction and Building Materials*, Vol. 335, 2022, id. 127482.

[7] Zheng, D., A. H. AlAteah, A. Alsubeai, and S. A. Mostafa. Integrating micro-and nanowaste glass with waste foundry sand in ultra-high-performance concrete to enhance material performance and sustainability. *Reviews on Advanced Materials Science*, Vol. 63, No. 1, 2024, id. 20240012.

[8] Ghafari, E., M. Arezoumandi, H. Costa, and E. Júlio. Influence of nano-silica addition on durability of UHPC. *Construction and Building Materials*, Vol. 94, 2015, pp. 181–188.

[9] Yu, R., P. Spiesz, and H. J. C. Brouwers. Development of an eco-friendly Ultra-High Performance Concrete (UHPC) with efficient cement and mineral admixtures uses. *Cement and Concrete Composites*, Vol. 55, 2015, pp. 383–394.

[10] Alkaysi, M., S. El-Tawil, Z. Liu, and W. Hansen. Effects of silica powder and cement type on durability of ultra high performance concrete (UHPC). *Cement and Concrete Composites*, Vol. 66, 2016, pp. 47–56.

[11] Muhd Norhasri, M. S., M. S. Hamidah, A. Mohd Fadzil, and O. Megawati. Inclusion of nano metakaolin as additive in ultra high performance concrete (UHPC). *Construction and Building Materials*, Vol. 127, 2016, pp. 167–175.

[12] Yalçınkaya, Ç. and H. Yazıcı. Effects of ambient temperature and relative humidity on early-age shrinkage of UHPC with high-volume mineral admixtures. *Construction and Building Materials*, Vol. 144, 2017, pp. 252–259.

[13] Li, P. P., Q. L. Yu, and H. J. H. Brouwers. Effect of PCE-type superplasticizer on early-age behaviour of ultra-high performance concrete (UHPC). *Construction and Building Materials*, Vol. 153, 2017, pp. 740–750.

[14] Shafieifar, M., M. Farzad, and A. Azizinamini. Experimental and numerical study on mechanical properties of Ultra High Performance Concrete (UHPC). *Construction and Building Materials*, Vol. 156, 2017, pp. 402–411.

[15] Zhang, X., X. Wu, X. Zhang, L. Wang, Y. Tang, F. J. C. Qiu, et al. Bond behaviors of pre-and post-yield deformed rebar embedded in ultra-high performance concrete. *Construction and Building Materials*, Vol. 341, 2022, id. 127839.

[16] Wang, J., Q. Dai, R. Si, Y. Ma, and S. Guo. Fresh and mechanical performance and freeze-thaw durability of steel fiber-reinforced rubber self-compacting concrete (SRSCC). *Journal of Cleaner Production*, Vol. 277, 2020, id. 123180.

[17] Ahmed, T. I., D. E. Tobbala, and B. Materials. Rubbered light concrete containing recycled PET fiber compared to macro-polypropylene fiber in terms of SEM, mechanical, thermal conductivity and electrochemical resistance. *Construction and Building Materials*, Vol. 415, 2024, id. 135010.

[18] Pham, T. M., Y. Y. Lim, and M. Malekzadeh. Effect of pre-treatment methods of crumb rubber on strength, permeability and acid

attack resistance of rubberised geopolymer concrete. *Journal of Building Engineering*, Vol. 41, 2021, id. 102448.
[19] Luhar, S., S. Chaudhary, and I. Luhar. Thermal resistance of fly ash based rubberized geopolymer concrete. *Journal of Building Engineering*, Vol. 19, 2018, pp. 420–428.
[20] Tang, Y., Y. Wang, D. Wu, M. Chen, L. Pang, J. Sun, et al. Exploring temperature-resilient recycled aggregate concrete with waste rubber: An experimental and multi-objective optimization analysis. *Reviews on Advanced Materials Science*, Vol. 62, No. 1, 2023, id. 20230347.
[21] Han, Y., Z. Lv, Y. Bai, G. Han, and D. J. P. Li. Experimental study on the mechanical properties of crumb rubber concrete after elevated temperature. *Polymers*, Vol. 15, No. 14, 2023, id. 3102.
[22] Salahaddin, S. D., J. H. Haido, and G. Wardeh. Rheological and mechanical characteristics of basalt fiber UHPC incorporating waste glass powder in lieu of cement. *Ain Shams Engineering Journal*, Vol. 15, No. 3, 2024, id. 102515.
[23] Salahaddin, S. D., J. H. Haido, and G. Wardeh. The behavior of UHPC containing recycled glass waste in place of cementitious materials: A comprehensive review. *Case Studies in Construction Materials*, Vol. 17, 2022, id. e01494.
[24] Lin, Y., W. Zhou, A. H. AlAteah, and S. A. Mostafa. Recycling and reuse of waste banded iron formation as fine aggregate in the production of lightweight foamed concrete: Fresh-state, mechanical, thermal, microstructure and durability properties assessment. *Construction and Building Materials*, Vol. 439, 2024, id. 137369.
[25] Samingthong, W., M. Hoy, B. Ro, S. Horpibulsuk, T. Yosthasaen, A. Suddeepong, et al. Natural rubber latex-modified concrete with PET and crumb rubber aggregate replacements for sustainable rigid pavements. *Sustainability*, Vol. 15, No. 19, 2023, id. 14147.
[26] Yuan, X., W. Xu, A. H. AlAteah, and S. A. Mostafa. Evaluation of the performance of high-strength geopolymer concrete prepared with recycled coarse aggregate containing eggshell powder and rice husk ash cured at different curing regimes. *Construction and Building Materials*, Vol. 434, 2024, id. 136722.
[27] Suddeepong, A., A. Buritatum, M. Hoy, S. Horpibulsuk, T. Takaikaew, J. Horpibulsuk, et al. Natural rubber latex–modified concrete pavements: evaluation and design approach. *Journal of Materials in Civil Engineering*, Vol. 34, No. 9, 2022, id. 04022215.
[28] AlAteah, A. H., K. A. A. Al-Sodani, M. O. Yusuf, A. A. Adewumi, M. M. Al-Tholaia, A. O. Bakare, et al. Modelling of strength characteristics of silica fume/glass ternary blended concrete using destructive and non-destructive testing methods. *Journal of Materials Research and Technology*, Vol. 22, 2023, pp. 997–1013.
[29] Du, B., F. Xu, A. H. AlAteah, and S. A. Mostafa. Sustainable development of ultra high-performance concrete using basil plant waste: Investigation at normal and extreme conditions. *Journal of Building Engineering*, Vol. 80, 2023, id. 107997.
[30] Zeyad, A. M., K. H. Bayagoob, M. Amin, B. A. Tayeh, S. A. Mostafa, and I. S. Agwa. Effect of olive waste ash on the properties of high-strength geopolymer concrete. *Structural Concrete*, 2024.
[31] Jagarapu, D. C. K. and A. Eluru. Strength and durability studies of lightweight fiber reinforced concrete with agriculture waste. *Materials Today: Proceedings*, Vol. 27, 2020, pp. 914–919.
[32] Mo, K. H., U. J. Alengaram, and M. Z. Jumaat. A review on the use of agriculture waste material as lightweight aggregate for reinforced concrete structural members. *Advances in Materials Science and Engineering*, Vol. 2014, 2014, pp. 1–9.
[33] Tayeh, B. A., A. A. Hakamy, M. S. Fattouh, and S. A. Mostafa. The effect of using nano agriculture wastes on microstructure and electrochemical performance of ultra-high-performance fiber reinforced self-compacting concrete under normal and acceleration conditions. *Case Studies in Construction Materials*, Vol. 18, 2023, id. e01721.
[34] Alnahhal, A. M., U. J. Alengaram, M. S. Ibrahim, S. Yusoff, H. S. C. Metselaar, and P. Gabriela Johnson. Synthesis of ternary binders and sand-binder ratio on the mechanical and microstructural properties of geopolymer foamed concrete. *Construction and Building Materials*, Vol. 349, 2022, id. 128682.
[35] Lynch, J. L. V., H. Baykara, M. Cornejo, G. Soriano, and N. A. Ulloa. Preparation, characterization, and determination of mechanical and thermal stability of natural zeolite-based foamed geopolymers. *Construction and Building Materials*, Vol. 172, 2018, pp. 448–456.
[36] Agwa, I. S., O. M. Omar, B. A. Tayeh, and B. A. Abdelsalam. Effects of using rice straw and cotton stalk ashes on the properties of lightweight self-compacting concrete. *Construction and Building Materials*, Vol. 235, 2020, id. 117541.
[37] Amin, M., A. M. Zeyad, B. A. Tayeh, and I. Saad Agwa. Effects of nano cotton stalk and palm leaf ashes on ultrahigh-performance concrete properties incorporating recycled concrete aggregates. *Construction and Building Materials*, Vol. 302, 2021, id. 124196.
[38] Joshaghani, A. and M. A. Moeini. Evaluating the effects of sugar cane bagasse ash (SCBA) and nanosilica on the mechanical and durability properties of mortar. *Construction and Building Materials*, Vol. 152, 2017, pp. 818–831.
[39] Neto, J. D., M. J. de França, N. S. de Amorim Júnior, and D. V. Ribeiro. Effects of adding sugarcane bagasse ash on the properties and durability of concrete. *Construction and Building Materials*, Vol. 266, 2021, id. 120959.
[40] Mello, L. C., M. A. dos Anjos, M. V. de Sá, N. S. de Souza, and E. C. de Farias. Effect of high temperatures on self-compacting concrete with high levels of sugarcane bagasse ash and metakaolin. *Construction and Building Materials*, Vol. 248, 2020, id. 118715.
[41] Agwa, I. S., A. M. Zeyad, B. A. Tayeh, and M. Amin. Effect of different burning degrees of sugarcane leaf ash on the properties of ultra-high-strength concrete. *Journal of Building Engineering*, Vol. 56, 2022, id. 104773.
[42] Kang, S. H., S. G. Hong, and J. Moon. The use of rice husk ash as reactive filler in ultra-high performance concrete. *Cement and Concrete Research*, Vol. 115, 2019, pp. 389–400.
[43] Chen, R., S. S. C. Congress, G. Cai, W. Duan, and S. Liu. Sustainable utilization of biomass waste-rice husk ash as a new solidified material of soil in geotechnical engineering: A review. *Construction and Building Materials*, Vol. 292, 2021, id. 123219.
[44] Mehta, A. and R. Siddique. Sustainable geopolymer concrete using ground granulated blast furnace slag and rice husk ash: Strength and permeability properties. *Journal of Cleaner Production*, Vol. 205, 2018, pp. 49–57.
[45] Van Tuan, N., G. Ye, K. van Breugel, A. L. A. Fraaij, and D. D. Bui. The study of using rice husk ash to produce ultra high performance concrete. *Construction and Building Materials*, Vol. 25, No. 4, 2011, pp. 2030–2035.
[46] Nair, D. G., A. Fraaij, A. A. K. Klaassen, and A. P. M. Kentgens. A structural investigation relating to the pozzolanic activity of rice husk ashes. *Cement and Concrete Research*, Vol. 38, No. 6, 2008, pp. 861–869.
[47] Santhosh, K. G., S. M. Subhani, and A. Bahurudeen. Recycling of palm oil fuel ash and rice husk ash in the cleaner production of concrete. *Journal of Cleaner Production*, Vol. 354, 2022, id. 131736.

[48] Al-Shwaiter, A., H. Awang, and M. A. Khalaf. Performance of sustainable lightweight foam concrete prepared using palm oil fuel ash as a sand replacement. *Construction and Building Materials*, Vol. 322, 2022, id. 126482.
[49] Kabir, S. M. A., U. J. Alengaram, M. Z. Jumaat, S. Yusoff, A. Sharmin, and I. I. Bashar. Performance evaluation and some durability characteristics of environmental friendly palm oil clinker based geopolymer concrete. *Journal of Cleaner Production*, Vol. 161, 2017, pp. 477–492.
[50] Amran, M., G. Murali, R. Fediuk, N. Vatin, Y. Vasilev, and H. Abdelgader. Palm oil fuel ash-based eco-efficient concrete: A critical review of the short-term properties. *Materials (Basel)*, Vol. 14, No. 2, 2021, id. 332.
[51] Ardiantoro, D., E. S. Sunarsih, and T. L. A. Sucipto. The role of rice husk ash in enhancing the fresh properties, density, and compressive strength of fly ash based self compacting geopolymer concrete. *Journal of Physics: Conference Series*, Vol. 1808, No. 1, 2021, id. 012014.
[52] Riyanto, A., S. Sembiring, S. Husain, R. S. Karimah, and I. Firdaus. Rietveld analysis of geopolymer prepared from amorphous rice husk silica with different thermal treatment. *Journal of Physics: Conference Series*, Vol. 1751, No. 1, 2021, id. 012070.
[53] Shen, Y. Rice husk silica derived nanomaterials for sustainable applications. *Renewable and Sustainable Energy Reviews*, Vol. 80, 2017, pp. 453–466.
[54] Venkatesan, R. P. and K. C. Pazhani. Strength and durability properties of geopolymer concrete made with ground granulated blast furnace slag and black rice husk ash. *KSCE Journal of Civil Engineering*, Vol. 20, No. 6, 2015, pp. 2384–2391.
[55] Tchakouté, H. K., D. E. Tchinda Mabah, C. Henning Rüscher, E. Kamseu, F. Andreola, M. C. Bignozzi, et al. Preparation of low-cost nano and microcomposites from chicken eggshell, nano-silica and rice husk ash and their utilisations as additives for producing geopolymer cements. *Journal of Asian Ceramic Societies*, Vol. 8, No. 1, 2020, pp. 149–161.
[56] Wu, J., Z. Zhang, Y. Zhang, and D. Li. Preparation and characterization of ultra-lightweight foamed geopolymer (UFG) based on fly ash-metakaolin blends. *Construction and Building Materials*, Vol. 168, 2018, pp. 771–779.
[57] Liang, G., T. Liu, H. Li, B. Dong, and T. Shi. A novel synthesis of lightweight and high-strength green geopolymer foamed material by rice husk ash and ground-granulated blast-furnace slag. *Resources, Conservation and Recycling*, Vol. 176, 2022, id. 105922.
[58] Ibrahim, W. M., K. Hussin, M. M. Abdullah, and A. A. Kadir. Geopolymer lightweight bricks manufactured from fly ash and foaming agent. *AIP Conference Proceedings*, Vol. 1835, 2017, id. 020048.
[59] Al Bakri Abdullah, M. M., Z. Yahya, M. F. Mohd Tahir, K. Hussin, M. Binhussain, and A. V. Sandhu. Fly ash based lightweight geopolymer concrete using foaming agent technology. *Applied Mechanics and Materials*, Vol. 679, 2014, pp. 20–24.
[60] Demiss, B. A., W. O. Oyawa, S. M. Shitote, and S. Benfratello. Mechanical and microstructural properties of recycled reactive powder concrete containing waste glass powder and fly ash at standard curing. *Cogent Engineering*, Vol. 5, No. 1, 2018, id. 1464877.
[61] Arora, A., M. Aguayo, H. Hansen, C. Castro, E. Federspiel, B. Mobasher, et al. Microstructural packing- and rheology-based binder selection and characterization for Ultra-high Performance Concrete (UHPC). *Cement and Concrete Research*, Vol. 103, 2018, pp. 179–190.
[62] Arora, A., A. Almujaddidi, F. Kianmofrad, B. Mobasher, and N. Neithalath. Material design of economical ultra-high performance concrete (UHPC) and evaluation of their properties. *Cement and Concrete Composites*, Vol. 104, 2019, id. 103346.
[63] Mostafa, S. A., A. S. Faried, A. A. Farghali, M. M. El-Deeb, T. A. Tawfik, S. Majer, et al. Influence of nanoparticles from waste materials on mechanical properties, durability and microstructure of UHPC. *Materials (Basel)*, Vol. 13, No. 20, 2020, id. 4530.
[64] Arora, A., Y. Yao, B. Mobasher, and N. Neithalath. Fundamental insights into the compressive and flexural response of binder- and aggregate-optimized ultra-high performance concrete (UHPC). *Cement and Concrete Composites*, Vol. 98, 2019, pp. 1–13.
[65] Mostafa, S. A., M. M. El-Deeb, A. A. Farghali, and A. S. Faried. Evaluation of the nano silica and nano waste materials on the corrosion protection of high strength steel embedded in ultra-high performance concrete. *Scientific Reports*, Vol. 11, No. 1, 2021, id. 2617.
[66] Huang, H., X. Gao, H. Wang, and H. Ye. Influence of rice husk ash on strength and permeability of ultra-high performance concrete. *Construction and Building Materials*, Vol. 149, 2017, pp. 621–628.
[67] Ribeiro, H., E. Vasconcelos, and J. Q. Dos Santos. Fertilisation of potted geranium with a municipal solid waste compost. *Bioresource Technology*, Vol. 73, No. 3, 2000, pp. 247–249.
[68] AlAteah, A. H. Engineering characteristics of ultra-high performance basalt fiber concrete incorporating geranium plant waste. *Case Studies in Construction Materials*, Vol. 19, 2023, id. e02618.
[69] Altaf, K., A. Younis, Y. Ramzan, and F. Ramzan. Effect of composition of agricultural wastes and biochar as a growing media on the growth of potted Stock (Matthiola incana) and Geranium (Pelargonium spp). *Journal of Plant Nutrition*, Vol. 44, No. 7, 2021, pp. 919–930.
[70] EN BSJLECFS. 197-1. *Cement–Part 1: Composition, specifications and conformity criteria for common cements*, European Committee for Standardization, 2011.
[71] Du, J., W. Meng, K. H. Khayat, Y. Bao, P. Guo, Z. Lyu, et al. New development of ultra-high-performance concrete (UHPC). *Composites Part B: Engineering*, Vol. 224, 2021, id. 109220.
[72] Lun Lam, W., P. Shen, Y. Cai, Y. Sun, Y. Zhang, and C. Sun Poon. Effects of seawater on UHPC: Macro and microstructure properties. *Construction and Building Materials*, Vol. 340, 2022, id. 127767.
[73] Luo, Q., Y.-Y. Wu, W. Qiu, H. Huang, S. Pei, P. Lambert, et al. Improving flexural strength of UHPC with sustainably synthesized graphene oxide. *Nanotechnology Reviews*, Vol. 10, No. 1, 2021, pp. 754–767.
[74] Ali, N., O. Canpolat, Y. Aygörmez, and M. M. Al-Mashhadani. Evaluation of the 12–24 mm basalt fibers and boron waste on reinforced metakaolin-based geopolymer. *Construction and Building Materials*, Vol. 251, 2020, id. 118976.
[75] Zhang, C., Y. Wang, X. Zhang, Y. Ding, and P. Xu. Mechanical properties and microstructure of basalt fiber-reinforced recycled concrete. *Journal of Cleaner Production*, Vol. 278, 2021, id. 123252.
[76] Yonggui, W., L. Shuaipeng, P. Hughes, and F. Yuhui. Mechanical properties and microstructure of basalt fibre and nano-silica reinforced recycled concrete after exposure to elevated temperatures. *Construction and Building Materials*, Vol. 247, 2020, id. 118561.
[77] Zheng, Y., J. Zhuo, and P. Zhang. A review on durability of nano-SiO2 and basalt fiber modified recycled aggregate concrete. *Construction and Building Materials*, Vol. 304, 2021, id. 124659.
[78] Wang, D., Y. Ju, H. Shen, and L. Xu. Mechanical properties of high performance concrete reinforced with basalt fiber and

polypropylene fiber. *Construction and Building Materials*, Vol. 197, 2019, pp. 464–473.

[79] Babalola, O. E., P. O. Awoyera, D. H. Le, and L. M. Bendezú Romero. A review of residual strength properties of normal and high strength concrete exposed to elevated temperatures: Impact of materials modification on behaviour of concrete composite. *Construction and Building Materials*, Vol. 296, 2021, id. 123448.

[80] Ozawa, M., S. Subedi Parajuli, Y. Uchida, and B. Zhou. Preventive effects of polypropylene and jute fibers on spalling of UHPC at high temperatures in combination with waste porous ceramic fine aggregate as an internal curing material. *Construction and Building Materials*, Vol. 206, 2019, pp. 219–225.

[81] Derinpinar, A. N., M. B. Karakoç, and A. Özcan. Performance of glass powder substituted slag based geopolymer concretes under high temperature. *Construction and Building Materials*, Vol. 331, 2022, id. 127318.

[82] Amin, M., I. Y. Hakeem, A. M. Zeyad, B. A. Tayeh, A. M. Maglad, and I. S. Agwa. Influence of recycled aggregates and carbon nanofibres on properties of ultra-high-performance concrete under elevated temperatures. *Case Studies in Construction Materials*, Vol. 16, 2022, id. e01063.

[83] Mahmoud, M. S., A. S. Shanour, G. E. Abdelaziz, and M. S. Hammad. Influence of elevated temperature on performance of ultra high strength fibre reinforced self compacting concrete (UHSFRSCC) produced from local materials. *Engineering Research Journal (Shoubra)*, Vol. 52, No. 1, 2023, pp. 1–11.

[84] Ziada, M., S. Erdem, Y. Tammam, S. Kara, and R. A. G. Lezcano. The effect of basalt fiber on mechanical, microstructural, and high-temperature properties of fly ash-based and basalt powder waste-filled sustainable geopolymer mortar. *Sustainability*, Vol. 13, No. 22, 2021, id. 12610.

[85] Shen, W., Y. Liu, L. Cao, X. Huo, Z. Yang, C. Zhou, et al. Mixing design and microstructure of ultra high strength concrete with manufactured sand. *Construction and Building Materials*, Vol. 143, 2017, pp. 312–321.

[86] Bahmani, H. and D. Mostofinejad. Microstructure of ultra-high-performance concrete (UHPC) – A review study. *Journal of Building Engineering*, Vol. 50, 2022, id. 104118.

[87] He, Z. H., S. G. Du, and D. Chen. Microstructure of ultra high performance concrete containing lithium slag. *Journal of Hazardous Materials*, Vol. 353, 2018, pp. 35–43.

[88] Li, T., Y. Zhang, and J. G. Dai. Flexural behavior and microstructure of hybrid basalt textile and steel fiber reinforced alkali-activated slag panels exposed to elevated temperatures. *Construction and Building Materials*, Vol. 152, 2017, pp. 651–660.

[89] Ma, Q. and Y. Zhu. Experimental research on the microstructure and compressive and tensile properties of nano-SiO_2 concrete containing basalt fibers. *Underground Space*, Vol. 2, No. 3, 2017, pp. 175–181.